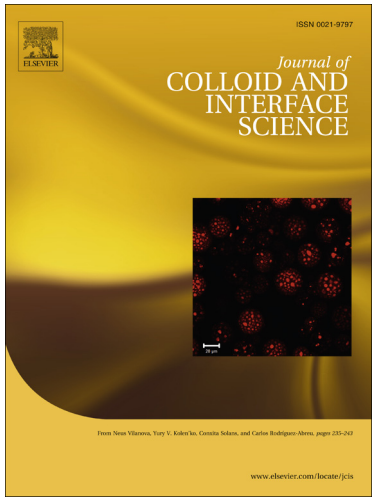

Does As(III) interact with Fe(II), Fe(III) and organic matter through ternary complexes?

Charlotte Catrouillet, Mélanie Davranche, Aline Dia, Martine Bouhnik-Le Coz, Edwige Demangeat, Gérard Gruau

PII: S0021-9797(16)30127-8
DOI: http://dx.doi.org/10.1016/j.jcis.2016.02.047
Reference: YJCIS 21109

To appear in: *Journal of Colloid and Interface Science*

Received Date: 8 January 2016
Revised Date: 18 February 2016
Accepted Date: 18 February 2016

Please cite this article as: C. Catrouillet, M. Davranche, A. Dia, M.B-L. Coz, E. Demangeat, G. Gruau, Does As(III) interact with Fe(II), Fe(III) and organic matter through ternary complexes?, *Journal of Colloid and Interface Science* (2016), doi: http://dx.doi.org/10.1016/j.jcis.2016.02.047

Does As(III) interact with Fe(II), Fe(III) and organic matter through ternary complexes?

Charlotte Catrouillet[a*], Mélanie Davranche[a], Aline Dia[a], Martine Bouhnik-Le Coz[a], Edwige Demangeat[a], Gérard Gruau[a]

[a] Géosciences Rennes UMR 6118, Université Rennes 1, CNRS, 35042 Rennes cedex, France

* Corresponding author: charlotte.catrouillet@univ-rennes1.fr, +33 (0)2 23 23 54 58

Keywords: Arsenic(III), Iron(II, III) humic substances, binding, sorption, PHREEQC-Model VI, PHREEPLOT, ternary complex

ABSTRACT

Up until now, only a small number of studies have been dedicated to the binding processes of As(III) with organic matter (OM) via ionic Fe(III) bridges; none was interested in Fe (II). Complexation isotherms were carried out with As(III), Fe(II) or Fe(III) and Leonardite humic acid (HA). Although PHREEQC/Model VI, implemented with OM thiol groups, reproduced the experimental datasets with Fe(III), the poor fit between the experimental and modeled Fe(II) data suggested another binding mechanism for As(III) to OM. PHREEQC/Model VI was modified to take various possible As(III)-Fe(II)-OM ternary complex conformations into account. The complexation of As(III) as a mononuclear bidentate complex to a bidentate Fe(II)-HA complex was evidenced. However, the model needed to be improved since the distribution of the bidentate sites appeared to be unrealistic with regards to the published XAS data. In the presence of Fe(III), As(III) was bound to thiol groups which are more competitive with regards to the low density of formed Fe(III)-HA complexes. Based on the new data and previously published results, we propose a general scheme describing the various As(III)-Fe-MO complexes that are able to form in Fe and OM-rich waters.

1 Introduction

Arsenic (As) is a strong contaminant of water and soil worldwide (Word Health organization), mainly as arsenite - As(III) - or arsenate - As(V) - depending on the redox conditions [1]. Iron (Fe) speciation exerts a strong control on the As fate in the environment, as oxidized Fe species are known for their capacity to bind high concentrations of As(III,V) [2,3]. Organic matter (OM) seems to be an important direct and indirect controlling factor, especially in floodplains and wetlands where As concentrations can be high [4–6]. Organic matter act (i) as a source of C for bacterial metabolic activity, especially Fe(III) and As(V) reducing-bacteria, (ii) as a sorbent of Fe(III,II)/Fe(III)-oxyhydroxides [7–11], and as an As(III, V) competitor for its binding to Fe(III)-oxyhydroxides [12–16]. More recently, several studies demonstrated that OM may directly bind As(III,V). Different mechanisms were put forward to describe As-OM binding, including As(III, V) complexation with OM carboxylic and phenolic groups [17,18], or As(III) binding with OM thiol groups [19–21]. However, most of the As bound to OM generally occurs as As-Fe-OM ternary complexes in several systems, such as peatland, riparian wetlands, streams, groundwaters [13,22–27]. The high affinity of As for Fe(III)-oxyhydroxides and of Fe(III)/Fe(III)-oxyhydroxides for OM explains this behavior [14,23,25,28–31]. These studies were predominantly performed under oxidizing conditions and therefore concerned As(V). The situation is much less clear regarding the possible predominance of As(III)-Fe-OM ternary complexes. Using SEC-ICP-MS coupling and ultrafiltration, some authors provided evidence that As(III) could also form ternary complexes with OM via Fe(III) bridges, even though they failed to identify the nature of the Fe(III) bridges: Fe(III) ions or Fe(III)-oxyhydroxides [31]. Hoffmann et al. [26] who studied the As(III) binding to natural peat via ionic Fe(III) showed an increasing binding with increasing Fe(III) concentrations. Using EXAFS records, they suggested that As(III) binding could occur either through mononuclear bidentate or binuclear monodentate complexes with Fe(III). They argued that the stability constants for ternary complexes were probably lower than those for the direct As(III) binding to peat thiol groups. However, the high experimental concentrations required for the XAS measurements were quite far off from those generally expected in the

environment, especially ionic Fe(III) concentrations which generally precipitate in such conditions. Finally, no study were interested in potential As(III) binding to OM via Fe(II), although these bridges are expected to be dominant in anoxic conditions, notably in wetlands and floodplains where OM, Fe and As concentrations are high [32].

The aim of this study was to evaluate the potentiality to form As(III)-Fe-OM ternary complexes via ionic Fe(II) and Fe(III) bridges at concentrations prevailing in natural waters. As a result, we developed a combined experimental and modeling approach to (i) discriminate between the controlling binding mechanisms involved in the formation of As(III)-Fe-OM ternary complexes and (ii) provide stability constants to quantify which of these mechanisms are likely to be dominant in natural waters. The major advantage of the modeling approach is to test mechanisms at lower Fe amounts than those required by spectroscopic methodologies.

2 Experimental section

2.1 Experimental setup

All of the aqueous solutions were prepared with analytical grade Milli-Q water. The As(III), Fe(II) and Fe(III) stock solutions were prepared with sodium arsenite ($NaAsO_2$), iron chloride tetrahydrate ($FeCl_2.4H_2O$) and iron nitrate nonahydrate ($Fe(NO_3)_3.9H_2O$), respectively. The used humic acid (HA) was the standard HA Leonardite from the International Humic Substance Society. It was purified by removing the HA molecules < 10 kDa using a Labscale TFF system equipped with a Pellicon XL membrane. The composition of the purified HA could be probably slightly modified by this purification as compared to the initial HA. All binding experiments (except Fe(III), see below) were conducted in a Jacomex isolator glove box (< 5 ppm of O_2) to prevent the oxidation of As(III) and Fe(II). The ionic strength was fixed at 0.05 M with NaCl for all experiments.

As(III)-Fe(II)-HA experiments. Three adsorption isotherm experiments were carried out at 50 mg L^{-1} DOC (dissolved organic carbon). The first adsorption isotherm was performed at pH 6 with 50 µg L^{-1} of As(III) and 0.8-12 mg L^{-1} of Fe(II). The second and third

isotherms were carried out at pH 6 and 5, respectively, with 5-50 µg L^{-1} of As(III) and 5-6 mg L^{-1} of Fe(II). Arsenic and Fe(II) solutions were added simultaneously to humic acid solution, and were then stirred for 48 h to reach equilibrium.

As(III)-Fe(III)-HA experiments. Three standard batch equilibrium experiments were carried out with DOC and Fe^{3+} concentrations of 50 and 0.5 mg L^{-1}, respectively. The Fe(III) stock solution was prepared at pH 1.5 and the Fe^{3+} concentration used was adjusted to prevent oxyhydroxide precipitation. Using PHREEQC-Model VI and the minteq.v4 database modified with respect to Fe(III)-HA binding [9,33], the model showed that precipitation was only expected to occur for Fe(III) concentrations > 1.2 mg L^{-1}. The pH was fixed at 4, 5 and 6 with sub boiling HCl and NaOH for the three isotherms, respectively. Experimental solutions were stirred for 24h to reach equilibrium between Fe^{3+} and HA. Arsenic(III) was added at concentrations ranging from 5 to 50 µg L^{-1} in a glove box to prevent oxidation. Experimental solutions were then stirred for 48h to reach equilibrium.

Sampling. For all experiments, 15 mL of solution was sampled and ultrafiltrated at 5 kDa (Vivaspin VS15RH12, Sartorius) under N_2 atmosphere. Ultracentrifugation cells were previously washed with Milli-Q water until DOC concentration in the ultrafiltrate was < 1 mg L^{-1}. All experiments were conducted in duplicate.

2.2 Chemical analyses

All measurements were performed at Géosciences Rennes, France. DOC concentrations were measured using an organic carbon analyzer (Shimadzu TOC-V CSH). Arsenic and Fe concentrations were determined using an ICP-MS. Instrumental and data acquisition parameters can be found in the Supporting Information 1 (SI). To ensure that no oxidation occurred during the experiments, the concentrations of As(III) and As(V) were monitored using a HPLC-Agilent 1260 Infinity coupled to an Agilent G3154-65001 and Fe_{TOT} was compared to the Fe(II) measured in the ultrafiltrate ($Fe(II)_{UF}$) using the 1.10-phenanthroline colorimetric method (AFNOR, 1982). Because the absorbance of Leonardite at 50 mg L^{-1} is high, the Fe(II) concentration in the Fe(II)-HA solution was not checked.

Arsenic(III) and Fe in the ultrafiltrates were assumed to be inorganic whereas As(III) and Fe bound to HA were considered to be in the fraction > 5 kDa.

2.3 Modeling

2.3.1 Model description

Because As(III) can bind to OM thiol groups, the modeling calculations were performed using a modified version of the PHREEQC/Model VI allowing this particular binding to be taken into account [21]. In the modified PHREEQC-Model VI, the ions complexation occurs through 12 discrete sites: four carboxylic groups (sites A), four phenolic groups (sites B) and four thiol groups (sites S). The abundances, intrinsic acidity constant for A, B and S sites and their distribution term are denoted as n_A, n_B, n_S, pK_A, pK_B, pK_S, ΔpK_A, ΔpK_B and ΔpK_S, respectively. Only monodentate complexes of As(III) with thiols are defined [21]. The fraction of proton sites that can form bidentate and tridentate complexes are named f_B and f_T, respectively [34]. All values of the parameters used for modeling calculations are given in supporting information Table S7. The strength of the interaction between one site and one ion is defined by the complexation constant log K. Considering the 12 sites that can generate bidentates and tridentates, 84 equations are needed to describe the interaction between one ion and the 84 HA sites (further information is given in section 2.2 of the supporting information). The specific complexation parameters for the carboxylic, phenolic and thiol groups are log K_{MA}, log K_{MB} and log K_{MS}, respectively. The CCM model was used to model the electrostatic interactions. Ion accumulation in the vicinity of HA is calculated with the Donnan model. Further information can be found elsewhere [21].

2.3.2 Binding parameters and modeling strategy

Binary complexes. The binding parameters describing As(III) complexation by HA were previously determined using modified PHREEQC/Model VI including As(III)-thiol complexes [21]. The binding parameters used for the Fe(II)-HA binary complexes were determined using an earlier PHREEQC/Model VI version without thiol groups implementation

[7]. These parameters therefore had to be re-evaluated using the present dataset and the new model version. To keep same proportions of monodentates, bidentates and tridentates the ΔLK_2 value used and the relationship between log K_{MA} and log K_{MB} were the same as those previously used [7], $\Delta LK_2 = 3.90$ and $\log K_{MA} = 0.49 * \log K_{MB}$. All binding parameters calculated here are presented in supporting information Table S 8. All equations describing Fe(II) binding with each OM site were described in a previous study [7].

Ternary complexes. The experimental data were fitted using the PHREEPLOT program coupled with the modified version of PHREEQC/Model VI [7]. The 84 sites, their acidity constants and the binding parameters for Fe(II) and As(III) were added into the "minteq.v4" database. No previous study exists on the binding of As(III) to Fe(II)-HA complexes. The nature of the complexes formed had to be deduced from our experimental dataset and/or literature data. Only one study was dedicated to the characterization of the binding mechanisms of As(III) to Fe(III) as ion bound to peat [26]. Using EXAFS records, this study showed that for low Fe(III) concentrations, As(III) bound with Fe(III) as mononuclear bidentate complexes, whereas for high Fe(III) concentrations, As(III) bound with Fe(III) either as mononuclear bidentate complexes or as binuclear monodentate complexes. Jönsson and Sherman [35] suggested the formation of binuclear monodentate complexes for As(III) binding to green rust, fougerite and magnetite. However, Ona-Nguema et al. [36] rejected this hypothesis and proposed the formation of As(III) polymers. Thoral et al. [37] suggested that As(III) might form binuclear monodentate complexes with $Fe(OH)_2$ oxides under anoxic conditions. With respect to Fe(II), the modeling calculations performed earlier showed that Fe(II) bound with OM mainly through bidentate complexes [7], confirming this spectroscopic data [26].

Based on these proposed mechanisms, the modified PHREEQC/Model VI was first tested without Fe ternary complexes. They were implemented only when the model failed to reproduce the experimental datasets. From the spectroscopic data, six O atoms are bound to both Fe(II) and Fe(III) as FeO_6 octahedra [36,38]. Furthermore, the distance between As(III) and Fe(III) when As(III) is bound to Fe(III) oxides as corner-sharing bidentate complexes is

between $d_{As(III)-Fe(III)}$ = 3.4-3.58 Å and $d_{As(III)-Fe(II)}$ = 3.51 Å for $Fe(OH)_2$ [36,38]. All the complex conformations for As(III)-Fe(II) were thus deduced from the As(III)-Fe(III) spectroscopic datasets. The complexation of As(III) to monodentate Fe(II)-OM complexes was described either as mononuclear bidentate complexes (Eq. 1) or as binuclear bidentate complexes (Eq. 2). With regards to the As(III) binding to bidentate Fe(II)-OM complexes, As(III) complexation was described either as mononuclear bidentate complexes (Eq. 3) or as binuclear bidentate complexes (Eq. 4). Although Fe(III)-OM tridentate complexes were calculated in Model VI, the possibility to form complexes with As(III) was low considering their negative charge.

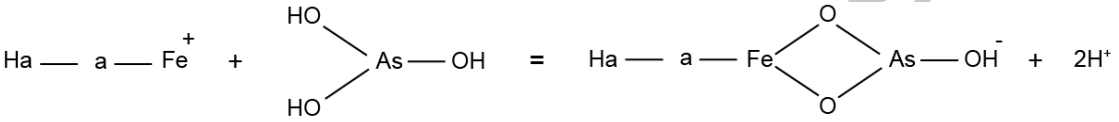

Eq. 1

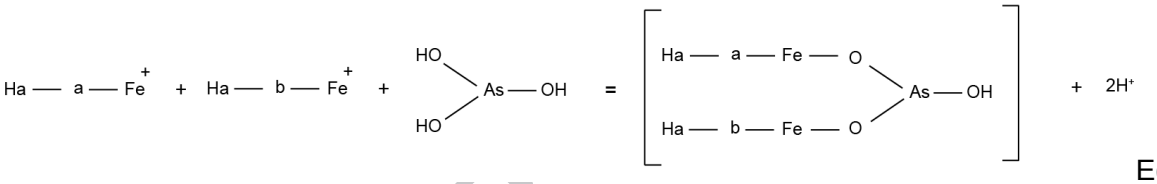

Eq. 2

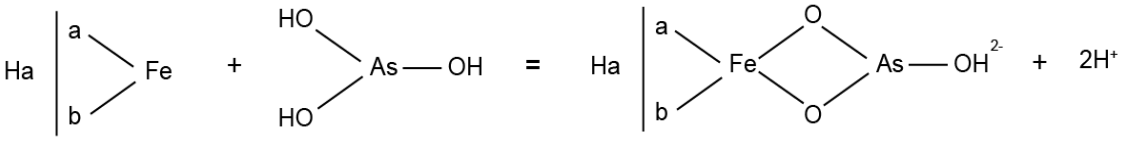

Eq. 3

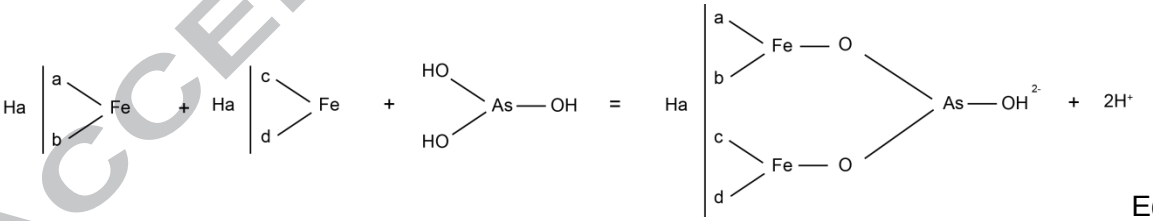

Eq. 4

All of these equations were first tested separately, then by pairs (i.e. Eqs. 1+2, or Eqs. 3+4), and last all together. All runs were finally compared to each other using their RMSE (Root Mean Square Deviation) calculated as $\sqrt{\mathrm{mean}((\log\mu(\mathrm{exp}) - \log\mu(\mathrm{cal}))^2}$, with logμ(exp) and logμ(cal) representing the logarithm of the measured and modeled As(III) bound concentrations, respectively.

3 Results

3.1 As(III)-Fe(II)-HA experimental and modeling data

No Fe(II) and As(III) oxidation occurred in the experiments. The binding parameters log K_{MA} (2.34) and log K_{MB} (4.78) for Fe(II) binding to HA, determined by fitting the experimental datasets using the modified PHREEQC/Model VI, were close to the log K_{MA} (2.19) and log K_{MB} (4.46) determined without the thiol sites implementation [7]. Since the relationship between log K_{MA}, log K_{MB} and ΔLK_2 was kept, the same proportions of monodentate, bidentate and tridentate complexes were calculated than previously [7]. Bidentates were the most abundant complexes formed between Fe(II) and HA. The experimental and modeled adsorption isotherm of Fe(II) binding to HA are presented in supporting information Figure S1.

The adsorption isotherms of As(III) by Fe(II)-HA (log[As(III)-HA] relative to log[$As(III)_{UF}$]) are displayed in Figure 1a, b and c. Figure 1a showed that, for the same As(III) concentrations but increasing Fe(II) concentrations, the amount of bound As(III) increased. For adsorption isotherms at pH 5 and 6, no plateau was reached, i.e. no saturation was obtained (Figure 1b and c). The model that did not take ternary complexes into account (e.g. As(III)-S-HA complexes) could not reproduce the experimental datasets (RMSE = 0.87). Therefore, the presence of Fe(II) modified the binding behavior of As(III) to HA and had to be taken into account in the model hypothesis. No Fe(II) oxides precipitated as evidenced by the saturation index calculated using PHREEQC/Model VI. Therefore, As(III) speciation was mainly controlled by direct As(III)-S-HA and indirect As(III)-Fe(II)-HA complexes.

Model fits obtained using one or more of the four equations described in section 2.3.2 are displayed in supporting information Figures S9-13. When only one equation was used, Eqs. 3 and 4 were the most reliable as shown by the low RMSE (RMSE = 0.18 and 0.19 respectively, Table 1 and Figures S5, 6). When a pair of equations were used (Eq. 1 + Eq. 2 or Eq. 3 + Eq. 4), the equation that yielded the smallest RMSE obtained in the single model (i.e. one equation) dominated the binding mechanism (Table 1). This result can be explained

by the fact that the fitting program works based on the smallest statistical parameters. When Fe(II) binding to HA was considered to occur via monodentate complexes, Eq. 1 dominated over Eq. 2, leading to a comparatively much higher log K: log K = 4.15 for Eq. 3 versus -1.33 for Eq. 2. Note that the log K obtained for Eq. 1 was similar to the one obtained with Eq. 1 only (Table 1). For the models that used both Eqs 3 and Eqs 4 (RMSE = 0.18, Table 1) and all equations together (supporting information Figure S8), the dominant equation was Eq. 3 (mononuclear bidentate complexation of As(III) with bidentate Fe(II)-HA complexes), with RMSE = 0.18.

The adsorption isotherms of As(III) to Fe(III)-HA (log[As(III)-HA] relative to log[$As(III)_{UF}$]) are displayed in Figure 1d, e and f. No plateau was reached at pH 5 and 6 (Figure 1e and f), by contrast with pH 4 (Figure 1d). The proportion of bound As(III) at the different pH was similar, suggesting a minor role of pH in As(III) binding. The model that only considered the binding of As(III) to thiol groups correctly reproduced the experimental data (Figure 1d, e and f and total RMSE = 0.52). The high RMSE was due to the dispersion of the experimental points. In our experimental conditions, Fe(III) did not seem to influence the binding of As(III) to HA.

4 Discussion

4.1 Monodentate or bidentate Fe(II)-HA sites: which ones complex As(III) most efficiently?

As shown by their lowest RMSE, Eqs. 3 and 4 better fit the experimental dataset (RMSE = 0.18 and 0.19, Table 1). However in PHREEQC/Model VI, the fraction of sites that can make bidentate Fe(II)-OM complexes was determined from the geometry of the OM molecules. The minimal distance between two sites was fixed at 0.3 nm for a sphere with a radius of 0.8 nm. If the distance between two sites ranged between 0.3 and 0.45 nm, the sites were defined as bidentate sites [39]. In our simulations, Eq. 4 represents the binding of As(III) to two Fe atoms, each forming bidentate complexes with OM. The distance between each Fe atom was $d_{Fe\text{-}Fe} \approx (0.3\text{-}0.45)*2 = 0.6\text{-}0.9$ nm = 6-9 Å (Figure 2a). Spectroscopic data

demonstrated that the distance between As and the neighbor O (d_{As-O}) varied from 1.70 to 1.79 Å [26,36,37,40]. The distance between Fe(III) and O atoms (d_{Fe-O}) varied from 1.94 to 1.99 Å [26,40] and from 1.99 to 2.14 Å for Fe(II)-O and Fe(II)-As(III) systems [36,37,41]. The maximal distance between As and Fe bound via an O ($d_{As-O-Fe}$) was therefore equal to $d_{As-O-Fe}max = d_{As-O}max + d_{Fe-O}max = 1.79 + 2.14 = 3.93$ Å which was << 6-9 Å (d_{Fe-Fe} for two bidentate sites). Thus, the binding of As to Fe through O with distances of 6-9 Å between two Fe atoms seemed impossible (Figure 2a). Therefore, although PHREEQC/Model VI allowed the binding of As(III) to HA through Fe(II) bidentate sites, for geometrical reasons, in experimental and natural conditions, this possibility was expected only when Fe dimer and trimer appeared [25,26,42,43].

Equation 2, which assumed the As(III) binding to two Fe(II)-MO monodentates, poorly reproduced the experimental datasets (RMSE = 0.58, Table 1). The fit was poor (RMSE = 0.71, supporting information Figure S3) for the isotherm at pH 5. According to PHREEQC-Model VI, the abundance of the Fe(II)-OM monodentate complexes would be quite low, ranging between 0.02 and 18% versus 74 and 83% for the Fe(II)-OM monodentate and bidentate complexes, respectively. This low abundance of the Fe(II)-OM monodentate complexes likely explained why Eq. 2 failed to satisfactorily reproduce the experimental data. A critical point was that in PHREEQC-Model VI, monodentate sites were assumed to be separated from each other by more than 4.5 Å whereas in the $Fe(OH)_2$ oxides, when As(III) was bound to Fe, d_{Fe-Fe} was smaller at 3.26 Å (Figure 2b). Therefore, Eq. 2 was impossible with the common hypothesis used in PHREEQC/Model VI. Hoffmann et al. [26] showed that As(III) could form binuclear monodentates with Fe(III) complexed to HA. As discussed above, the complexation of As(III) by bidentate Fe(II)-OM complexes was not reliable for geometrical reasons and as a result, only Fe(II)-OM monodentate could bind As(III). These observations suggested that a part of the bidentate sites, defined in the model as spaced apart by 3 to 4.5 Å, possibly bound Fe(II) in a monodentate mode (e.g. Ha-ab$(Fe)_2$ versus Ha-abFe).

Hoffmann et al. [26] showed that As(III) was bound as binuclear monodentate complexed to Fe(III)-OM. Using PHREEQC/Model VI and their experimental conditions, we

calculated that Fe(III) was able to recover between 0.75 and 5.95% of the HA sites. The coupling of the spectroscopic [26] and modeled datasets demonstrated that As(III) binuclear monodentate complexes were formed from a recovery of 5.95%. In our experiments, the surface recovery by Fe(II) ranged between 5 and 38% which support our hypothesis that As(III) binding to HA mainly occurred through binuclear monodentate Fe(II)-HA complexes.

Although Eq. 1 better reproduced the experimental datasets than Eq. 2, the calculated RMSE was higher than for Eqs. 3 and 4 (Table 1). Considering only the atomic distances, the binding of As(III) to only one Fe(II)-HA complex is thought to be plausible, but in addition, for example, to Eq. 3.

As seen previously, when several equations were used together, the model chose the equation that provided the smallest RMSE and attributed a negative log K to the other equations. With regards to the Fe(II) recovery on HA, and the spectroscopic data in the literature, mononuclear bidentate and binuclear monodentate complexes seemed to be the most reliable mechanisms involved in As(III) binding by Fe(II)-HA. Used together Eqs. 1 and 2 described the As(III) binding to Fe(II)-HA monodentate complexes. Regarding the low density of Fe(II)-HA monodentates, the model should be able to determine the log K for both equations. When Eqs. 3 and 4 were used together, enough Fe(II) bidentate complexes were formed. However, none of these coupled equations reasonably fit the experimental datasets. In fact, the model was not able to assess the respective weight of each equation. Some constraints had to be implemented in PHREEQC/Model VI to improve the quantification of each equation relative to the other ones. PHREEQC/Model VI was able to accurately discriminate the binding of one ion to the carboxylic and phenolic sites and to determine the corresponding binding parameters. In this case, the constraints were imposed by the acidity constants which control the density of each site relative to the pH and by the imposed linear relationship between the log K_{MA} and log K_{MB} values (log K_{MB} = 3.39 * log K_{MA}) [34].

4.2 Instructions to better model As(III)-Fe(II)-HA interactions

To improve the modeling of the data using Eq. 2 – the most probable equation with regards to the spectroscopic data [26] - we modified PHREEQC/Model VI by identifying the proportion of bidentate sites that can potentially bind two Fe (2-monodentate mode). In Model VI, the bidentate Fe(II) sites are distributed between weak, strong, and very strong bidentate sites. The differences between each site are defined by the site abundance and the ion binding parameters (log K_{MA}, log K_{MB} and ΔLK_2). The strong and very strong bidentate sites are 10.01 and 100.11 times less abundant, respectively, than the weak bidentate site. The log K value for the strong bidentate sites is equal to that of the weak bidentate sites plus ΔLK_2, the distribution term that modified the strength of the bidentate and tridentate sites. Log K for the very strong bidentate sites are equal to those for weak bidentate sites plus $2*\Delta LK_2$. In a bidentate complex, two sites bind one Fe, whereas in the 2-monodentate mode, for each monodentate site, one site binds Fe. In the 2-monodentate mode, log K will be lower than the bidentate log K. Therefore, the 2-monodentate could only be developed from the weak bidentate group, as strong and very strong bidentate sites have higher binding constants. In PHREEQC/Model VI, the binding constant for the weak bidentate group was defined as the sum of two monodentate sites; however, the mechanism had to be modified to correspond to the required 2-monodentate mode. Equation 5 corresponds to the classical equation and Eq. 6 to the equation for the 2-monodentate mode.

$Ha\_ab^{2-} + Fe^{2+} = Ha\_abFe$ log k = logk(a) + logk(b) (Eq. 5)

$Ha\_ab^{2-} + 2Fe^{2+} = Ha\_abFe_2^{+2}$ log k = logk(a) + logk(b) (Eq. 6)

With regards to the abundance of the sites, it cannot be assumed that all of the weak bidentate sites are involved in the 2-monodentate mode. It was also difficult to quantify the exact proportion of weak bidentate sites that could bind Fe(II) in the 2-monodentate mode. Consequently, tests were performed with a proportion of these weak bidentate sites varying from 5 to 90%. When the proportion was 5%, 5% of the weak bidentate sites bound Fe following Eq. 2 and 95% following Eq. 3 when fitting the experimental data (supporting information Table S13). This procedure was applied to Eqs. 2 and 3 simultaneously, which corresponded to a new modeling configuration. The model was not able to determine the log

K for the proportions ranging from 5 to 80%. However, for 90% of the bidentate sites that used Eq. 3, the fitted log K were equal to 2.86 and 3.95, respectively. Because As(III) was only bound to one Fe following this equation versus two Fe in Eq. 2, the log K for Eq. 2 should be lower than for Eq. 3; 90% of the bidentate sites that used the 2-monodentate mode were therefore too large. Thus, it is necessary to experimentally/analytically determine the proportions of Fe(II) among the bidentate sites that could possibly be involved in the 2-monodentate mode (e.g. using spectroscopy). Then, log K between As(III) and the Fe(II)-HA complexes should be determined using both binding mechanisms.

4.3 Interpretation of the As(III)-Fe(III)-HA data

The model using thiol groups only reproduced our experimental datasets reasonably well. The presence of Fe(III) did not seem to influence the binding of As(III) to the thiol groups, suggesting that (i) no competition for thiol groups occurred and (ii) no or negligible ternary complexes were formed. However, for their experimental conditions, Hoffmann et al. [26] clearly observed this type of ternary associations between As(III), Fe(III) and peat. The reason was that the concentrations used were much higher (in [26] 13 g L^{-1}, 20-200 mg L^{-1} and 22.5 mg L^{-1} of DOC, Fe(III) and As(III), respectively versus, here, 50 mg L^{-1}, 0.6 mg L^{-1} and 5-50 µg L^{-1} of DOC, Fe(III) and As(III), respectively), and the pH was different (pH 7, 8.4 and 8.8 [26] versus 4, 5 and 6 here). At pH 8.4 and 8.8, As(III) occurred as $H_2AsO_3^-$ implying the formation of new complex. The negative charge caused by the higher pH increased the binding of As(III) as ternary complexes via Fe(III) bridges as shown by the comparison of the isotherms performed for similar Fe(III) and As(III) concentrations but different pH in Hoffmann et al. (Figure 2A in [26]). Although the DOC/Fe ratios were equivalent (65-650 for [26] and 83 here), the As/Fe ratios were different (1.1-0.11 for [26] versus 0.0083-0.001 here). Moreover, the Fe(III) concentrations used here were chosen to avoid any Fe(III) precipitation. The S content of the peat used by Hoffmann et al. [26] was also very low and did not allow the binding of As(III) to peat through thiol sites, by contrast, with the here used HA as previously shown [21]. Thus, the thiol sites were able to compete with the Fe(III)-HA complexes, in low

amounts, for As(III) binding. At circumneutral pH and intermediate As/C ratio, Hoffmann et al. [26] observed that the log Kd (distribution coefficient of As(III) on organic carbon) was higher for As(III) bound to peat thiol sites than for As(III) bound to Fe(III)-peat complexes. In our experiments, As(III) bound to Fe(III)-HA was probably not present in high enough amounts to be detected, particularly in comparison with As(III) bound to S-HA. However, higher concentrations of Fe(III) should induce precipitation and the mechanism would be then performed with particulate or colloidal Fe(III) oxyhydroxides, which was not the purpose of the present study. It is important to note that the experimental conditions used by Hoffmann et al. [26] were developed to specifically promote the formation of ternary complexes via ionic Fe(III) and to allow the detection of As(III) and Fe(III) using the XAS technique.

4.4 Environmental implications

In floodplains and wetlands, the speciation of the elements depends strongly on the redox conditions. In such environments, when the soils are flooded and become water saturated, O_2 is consumed by bacteria, creating anoxic conditions, whereas when the soils are not saturated, oxic conditions prevailed. Under reducing conditions, As is mainly as As(III) and Fe as Fe(II), while under moderately reducing conditions As(III), As(V), Fe(II) and Fe(III) species can coexist. The speciation of Fe(III) depends on the amount of Fe(III) and on the physico-chemical conditions (pH, Eh, OM, competitors, etc.). For high Fe(III) concentrations, Fe occurs mostly as particulate or colloidal oxyhydroxides (lepidocrocite, ferrihydrite, goethite, etc.) generally bound to OM in organic-rich environments [44]. Iron(III) oxyhydroxides are the main sorbent of As(III) and As(V) in the environment. These systems are well documented and log K estimates can be found (Hfo_sOH + H_3AsO_3 = Hfo_sH_2AsO_3 + H_2O, log k = 5.41, 5.74 or 4.02 [2,3,45]). In organic-rich environments, As(III) is expected to either compete with OM molecules for its binding to Fe(III) oxyhydroxydes, which could strongly limit its complexation [13], or to be complexed by Fe(III) oxyhydroxides which are themselves bound to OM (Figure 3) [13,23,30,31]. For low Fe(III) concentrations, no precipitation occurred and Fe occurs as Fe^{3+}, $Fe(OH)^{2+}$ and $Fe(OH)_2^{+}$, depending on the pH.

In organic-rich environments, Fe(III) as ion can be bound by the carboxylic and phenolic groups of OM [8–10,43], mostly as bidentate complexes. Hoffmann et al. [26] showed that at high concentrations of Fe(III), As(III) and OM, ternary complexes can be produced via ionic Fe(III) (Figure 3). However, these results were strongly dependent on their experimental conditions performed to specifically promote this binding mechanism. In environmental conditions, for high amounts of Fe(III) such as those used by Hoffmann et al. [26], Fe(III) precipitated as Fe(III) oxyhydroxides and thus sorbed As(III) (high log K). In this case, we can consider that the ternary complex occurred through Fe(III) oxides or nano-oxides. In our studies, for higher OM thiol amounts and low Fe(III) concentrations, As(III)-Fe(III)-OM ternary complexes via ionic Fe(III) were not detected. Therefore, for an environmental level of Fe(III), ternary complexes via ionic Fe(III) does not seem possible even in organic-rich waters [44,46–48], notably when there is a sufficient number of thiol sites on OM to bind As(III) [19,21]. If the S% in OM does not totally correspond to thiol, much of the dissolved OM should contain a sufficiently high number of thiol groups to efficiently outcompete As(III) complexation by ternary Fe(III)-HA complexes. The competition between thiol binding and ternary complexes via ionic Fe(III) probably always occurs in natural OM-mediated interactions.

In waterlogged floodplains and wetlands, ferric-reducing bacteria reductively dissolved Fe(III) oxyhydroxides, thereby releasing Fe(II) into the solution. In such environments, high OM concentrations are produced. Catrouillet et al. [7] demonstrated that OM can strongly bind Fe^{2+} and $Fe(OH)^{+}$, especially at neutral and basic pH. Here, we showed that As(III) might be indirectly bound as ternary complexes to OM via ionic Fe(II) (Figure 3) and directly bound through OM thiol sites. The dynamics of the As(III) bound to OM is therefore controlled by the own OM dynamic. However, in the present work, we estimated that As(III) bound to OM by direct and indirect mechanisms could vary from 5% to 26% of the total As(III). We performed speciation calculations to test the studied mechanism in reduced water produced by the anoxic incubation of an organic-rich wetland soil (unpublished data). Arsenic(III), Fe(II) and DOC concentrations were measured in the

colloidal fraction which corresponded to the concentrations measured by ultrafiltration in the > 3kDa fraction, and the truly dissolved concentrations which corresponded to the concentrations measured by HPLC-ICP-MS in the < 3kDa fraction. In these calculations, we considered that the As(III) measured by HPLC-ICP-MS occurred as free species. This experimental dataset was used to test the present model using the following assumptions: DOC was only composed of HA (for which the proportion of reactive and non-reactive DOM was not known), the thiol groups concentration was equal to that of the Leonardite (0.13 mmol g^{-1}) and the binding of As(III) to Fe(II)-HA complexes was calculated using only Eq. 2, with log K = 3.39. We calculated that 1.2% of As(III) was bound to S-OM and 22.7% to Fe(II)-OM. These calculations were close to the proportion determined from the analytical techniques, i.e. 32% of As(III) bound to OM. The experimental proportions corresponded to the difference between As_{TOT} (determined by ICP-MS) and free As(III) concentrations (determined by HPLC-ICP-MS). Therefore, the binding of As(III) with OM as ternary complexes via ionic Fe(II) seemed to be potentially important in anoxic environments such as floodplains and wetlands, even if the mechanisms and binding constants used for this calculation had to be improved. As long as reducing conditions prevail, a large proportion (this study > 24-32%) of As(III) was in the solution as labile species, possibly transferred to the underlying aquifers.

Note that all of these complex conformations investigated in this study were described for the $As(OH)_3$ species. However, for pH > 8, As(III) is expected to occur as a negatively charged species, namely $As(OH)_3O$. Hoffmann et al. showed that with increasing pH, As(III) speciation change should result in a higher proportion of As(III) bound to OM through ternary complexes [26]. However, although the binding of ternary complexes seems to be favored for $As(OH)_2O^-$, few natural waters have pH > 8 and high enough OM and Fe concentrations. This is why these mechanisms were not presented in Figure 3.

5 Conclusion and perspectives

We provided experimental datasets for As(III) binding to HA as ionic Fe(II) and Fe(III) occurred. Arsenic(III) was bound to HA as ternary complexes via ionic Fe(II) and through HA thiol sites (4 to 26% of total As(III)). No ternary complexes seem to be formed with Fe(III) in our experimental conditions chosen to mimic natural waters Fe(III) and DOM concentrations. However, Hoffmann et al. [26], demonstrated the formation of such a complex. As assessed by EXAFS record, they showed that As(III) formed mononuclear bidentate and binuclear monodentate complexes, Fe(III) being itself bound to peat. The differences outlined in between both studies is explained by the lower Fe(III) concentrations and the higher amount of HA thiol groups in our experimental conditions. It appeared that Fe(III)-HA complex was not enough competitive regards to thiol functional group to succeed in As(III) binding at low Fe(III) concentrations. Various complex conformations were indeed tested with PHREEPLOT-PHREEQC/Model VI: (i) mononuclear bidentate of As(III) bound to monodentate of Fe(II) with OM, (ii) binuclear monodentate of As(III) bound to monodentate of Fe(II) with OM, (iii) mononuclear bidentate of As(III) bound to bidentate of Fe(II) to OM (iv) monodentate binuclear of As(III) to bidentate of Fe(II) to OM. The complex conformation involving binuclear monodentate of As(III) bound to bidentate of Fe(II) with OM was not possible regards to the atomic distances, deduced from the spectroscopic data available in literature and to their abundances. The complex conformation involving mononuclear bidentate of As(III) bound to bidentate of Fe(II) with OM was possible and fitted well the experimental datasets. The binding conformation based on binuclear monodentate of As(III) bound to monodentate of Fe(II) with OM was impossible in its current form with PHREEQC/Model VI. The atomic distances required a new binding mode for the bidentate sites described by Tipping [34], namely the formation of Fe(II) 2-monodentate complexes in the group of weak bidentates sites. PHREEQC/Model VI was not able actually to correctly model ternary complexes. Finally, the binding conformation involving mononuclear bidentate of As(III) bound to monodentate of Fe(II) with OM was possible but, unfortunately did not

correctly fit the experimental data. Even if ternary complexes were possible using ionic Fe(III, II), the percentage of As(III) bound to OM remained low. Most part of As(III) stayed labile and therefore is easily transferable to environment. The amount of As(III) bound to OM is however less mobile and its ability to be transferred in environment will depend on which in between particulate or colloidal OM this species is bound to. These results raise now the crucial question of the fate of this As(III) either labile or bound to OM when the conditions become oxidizing?

6 Acknowledgments

We are thankful to Dr. Rémi Marsac and Christian le Carlier de Veslud for advice regarding the modeling. Patrice Petitjean is acknowledged for ensuring the maintenance of the glove box during the experiments. Dr. Sara Mullin is thanked for post-editing the English style. This study was funded by the French ANR, through the “Programme Jeunes Chercheurs”: ARSENORG.

References

[1] J.A. Plant, D.G. Kinniburgh, P.L. Smedley, F.M. Fordyce, Arsenic and Selenium, in: Treatise Geochem., Elsevier, 2004: pp. 17–66.

[2] S. Dixit, J.G. Hering, Comparison of Arsenic(V) and Arsenic(III) Sorption onto Iron Oxide Minerals: Implications for Arsenic Mobility, Environ. Sci. Technol. 37 (2003) 4182–4189. doi:10.1021/es030309t.

[3] D.A. Dzombak, F.M.M. Morel, Surface Complexation Modeling, New York, 1990.

[4] W.P. Tseng, H.M. Chu, S.W. How, J.M. Fong, C.S. Lin, S. Yeh, Prevalence of skin cancer in an endemic area of chronic arsenicism in Taiwan, J. Natl. Cancer Inst. 40 (1968) 453.

[5] K. Kalbitz, R. Wennrich, Mobilization of heavy metals and arsenic in polluted wetland soils and its dependence on dissolved matter, Sci. Total Environ. 209 (1998) 27–39.

[6] H.M. Anawar, J. Akai, K. Komaki, H. Terao, T. Yoshioka, T. Ishizuka, et al., Geochemical occurrence of arsenic in groundwater of Bangladesh: sources and mobilization processes, J. Geochem. Explor. 77 (2003) 109–131. doi:10.1016/S0375-6742(02)00273-X.

[7] C. Catrouillet, M. Davranche, A. Dia, M. Bouhnik-Le Coz, R. Marsac, O. Pourret, et al., Geochemical modeling of Fe(II) binding to humic and fulvic acids, Chem. Geol. 372 (2014) 109–118. doi:10.1016/j.chemgeo.2014.02.019.

[8] T. Karlsson, P. Persson, Coordination chemistry and hydrolysis of Fe(III) in a peat humic acid studied by X-ray absorption spectroscopy, Geochim. Cosmochim. Acta. 74 (2010) 30–40. doi:10.1016/j.gca.2009.09.023.

[9] R. Marsac, M. Davranche, G. Gruau, A. Dia, M. Pédrot, M. Le Coz-Bouhnik, et al., Effects of Fe competition on REE binding to humic acid: Origin of REE pattern variability in organic waters, Chem. Geol. 342 (2013) 119–127. doi:10.1016/j.chemgeo.2013.01.020.

[10] C. Sjöstedt, I. Persson, D. Hesterberg, D.B. Kleja, H. Borg, J.P. Gustafsson, Iron speciation in soft-water lakes and soils as determined by EXAFS spectroscopy and geochemical modelling, Geochim. Cosmochim. Acta. 105 (2013) 172–186. doi:10.1016/j.gca.2012.11.035.

[11] H. Van Dijk, Cation binding of humic acids, Geoderma. 5 (1971) 53–67.

[12] H.J. Shipley, S. Yean, A.T. Kan, M.B. Tomson, A sorption kinetics model for arsenic adsorption to magnetite nanoparticles, Environ. Sci. Pollut. Res. 17 (2010) 1053–1062. doi:10.1007/s11356-009-0259-5.

[13] M. Grafe, M.J. Eick, P.R. Grossl, Adsorption of arsenate (V) and arsenite (III) on goethite in the presence and absence of dissolved organic carbon, Soil Sci. Soc. Am. J. 65 (2001) 1680–1687.

[14] M. Bauer, C. Blodau, Mobilization of arsenic by dissolved organic matter from iron oxides, soils and sediments, Sci. Total Environ. 354 (2006) 179–190. doi:10.1016/j.scitotenv.2005.01.027.

[15] S. Wang, C.N. Mulligan, Speciation and surface structure of inorganic arsenic in solid phases: A review, Environ. Int. 34 (2008) 867–879. doi:10.1016/j.envint.2007.11.005.

[16] M. Martin, L. Celi, E. Barberis, A. Violante, L.M. Kozak, P.M. Huang, Effect of humic acid coating on arsenic adsorption on ferrihydrite-kaolinite mixed systems, Can. J. Soil Sci. 89 (2009) 421–434.

[17] J. Buschmann, A. Kappeler, U. Lindauer, D. Kistler, M. Berg, L. Sigg, Arsenite and arsenate binding to dissolved humic acids: Influence of pH, type of humic acid, and aluminum, Environ. Sci. Technol. 40 (2006) 6015–6020.

[18] V. Lenoble, D.H. Dang, M. Loustau Cazalet, S. Mounier, H.-R. Pfeifer, C. Garnier, Evaluation and modelling of dissolved organic matter reactivity toward AsIII and AsV – Implication in environmental arsenic speciation, Talanta. 134 (2015) 530–537. doi:10.1016/j.talanta.2014.11.053.
[19] M. Hoffmann, C. Mikutta, R. Kretzschmar, Bisulfide Reaction with Natural Organic Matter Enhances Arsenite Sorption: Insights from X-ray Absorption Spectroscopy, Environ. Sci. Technol. 46 (2012) 11788–11797. doi:10.1021/es302590x.
[20] P. Langner, C. Mikutta, R. Kretzschmar, Arsenic sequestration by organic sulphur in peat, Nat. Geosci. 5 (2011) 66–73. doi:10.1038/ngeo1329.
[21] C. Catrouillet, M. Davranche, A. Dia, M. Bouhnik-Le Coz, M. Pédrot, R. Marsac, et al., Thiol groups controls on arsenite binding by organic matter: New experimental and modeling evidence, J. Colloid Interface Sci. 460 (2015) 310–320. doi:10.1016/j.jcis.2015.08.045.
[22] M. Bauer, C. Blodau, Arsenic distribution in the dissolved, colloidal and particulate size fraction of experimental solutions rich in dissolved organic matter and ferric iron, Geochim. Cosmochim. Acta. 73 (2009) 529–542. doi:10.1016/j.gca.2008.10.030.
[23] I. Ko, J.-Y. Kim, K.-W. Kim, Arsenic speciation and sorption kinetics in the As–hematite–humic acid system, Colloids Surf. Physicochem. Eng. Asp. 234 (2004) 43–50. doi:10.1016/j.colsurfa.2003.12.001.
[24] A.D. Redman, D.L. Macalady, D. Ahmann, Natural Organic Matter Affects Arsenic Speciation and Sorption onto Hematite, Environ. Sci. Technol. 36 (2002) 2889–2896. doi:10.1021/es0112801.
[25] C. Mikutta, R. Kretzschmar, Spectroscopic Evidence for Ternary Complex Formation between Arsenate and Ferric Iron Complexes of Humic Substances, Environ. Sci. Technol. 45 (2011) 9550–9557. doi:10.1021/es202300w.
[26] M. Hoffmann, C. Mikutta, R. Kretzschmar, Arsenite Binding to Natural Organic Matter: Spectroscopic Evidence for Ligand Exchange and Ternary Complex Formation, Environ. Sci. Technol. 47 (2013) 12165–12173. doi:10.1021/es4023317.
[27] E. Neubauer, F. von der Kammer, K.-H. Knorr, S. Peiffer, M. Reichert, T. Hofmann, Colloid-associated export of arsenic in stream water during stormflow events, Chem. Geol. 352 (2013) 81–91. doi:10.1016/j.chemgeo.2013.05.017.
[28] H.-T. Lin, M.. Wang, G.-C. Li, Complexation of arsenate with humic substance in water extract of compost, Chemosphere. 56 (2004) 1105–1112. doi:10.1016/j.chemosphere.2004.05.018.
[29] K. Ritter, G. Aiken R., J.F. Ranville, M. Bauer, D.L. Macalady, Evidence for the Aquatic Binding of Arsenate by Natural Organic Matter−Suspended Fe(III), Environ. Sci. Technol. 40 (2006) 5380–5387. doi:10.1021/es0519334.
[30] P. Sharma, M. Rolle, B. Kocar, S. Fendorf, A. Kappler, Influence of Natural Organic Matter on As Transport and Retention, Environ. Sci. Technol. 45 (2011) 546–553. doi:10.1021/es1026008.
[31] G. Liu, A. Fernandez, Y. Cai, Complexation of Arsenite with Humic Acid in the Presence of Ferric Iron, Environ. Sci. Technol. 45 (2011) 3210–3216. doi:10.1021/es102931p.
[32] M. Davranche, A. Dia, M. Fakih, B. Nowack, G. Gruau, G. Ona-nguema, et al., Organic matter control on the reactivity of Fe(III)-oxyhydroxides and associated As in wetland soils: A kinetic modeling study, Chem. Geol. 335 (2013) 24–35. doi:10.1016/j.chemgeo.2012.10.040.
[33] R. Marsac, M. Davranche, G. Gruau, M. Bouhnik-Le Coz, A. Dia, An improved description of the interactions between rare earth elements and humic acids by modeling:

PHREEQC-Model VI coupling, Geochim. Cosmochim. Acta. 75 (2011) 5625–5637. doi:10.1016/j.gca.2011.07.009.
[34] E. Tipping, Humic ion-binding model VI: an improved description of the interactions of protons and metal ions with humic substances, Aquat. Geochem. 4 (1998) 3–47.
[35] J. Jönsson, D.M. Sherman, Sorption of As(III) and As(V) to siderite, green rust (fougerite) and magnetite: Implications for arsenic release in anoxic groundwaters, Chem. Geol. 255 (2008) 173–181. doi:10.1016/j.chemgeo.2008.06.036.
[36] G. Ona-Nguema, G. Morin, Y. Wang, N. Menguy, F. Juillot, L. Olivi, et al., Arsenite sequestration at the surface of nano-Fe(OH)2, ferrous-carbonate hydroxide, and green-rust after bioreduction of arsenic-sorbed lepidocrocite by Shewanella putrefaciens, Geochim. Cosmochim. Acta. 73 (2009) 1359–1381. doi:10.1016/j.gca.2008.12.005.
[37] S. Thoral, J. Rose, J.M. Garnier, A. Van Geen, P. Refait, A. Traverse, et al., XAS study of iron and arsenic speciation during Fe (II) oxidation in the presence of As (III), Environ. Sci. Technol. 39 (2005) 9478–9485.
[38] G. Ona-Nguema, G. Morin, F. Juillot, G. Calas, G.E. Brown, EXAFS Analysis of Arsenite Adsorption onto Two-Line Ferrihydrite, Hematite, Goethite, and Lepidocrocite, Environ. Sci. Technol. 39 (2005) 9147–9155. doi:10.1021/es050889p.
[39] E. Tipping, M.A. Hurley, A unifying model of cation binding by humic substances, Geochim. Cosmochim. Acta. 56 (1992) 3627–3641.
[40] L.K. ThomasArrigo, C. Mikutta, J. Byrne, K. Barmettler, A. Kappler, R. Kretzschmar, Iron and Arsenic Speciation and Distribution in Organic Flocs from Streambeds of an Arsenic-Enriched Peatland, Environ. Sci. Technol. 48 (2014) 13218–13228. doi:10.1021/es503550g.
[41] T. Echigo, M. Kimata, Single-crystal X-ray diffraction and spectroscopic studies on humboldtine and lindbergite: weak Jahn–Teller effect of Fe2+ ion, Phys. Chem. Miner. 35 (2008) 467–475. doi:10.1007/s00269-008-0241-7.
[42] J.W.J. van Schaik, I. Persson, D.B. Kleja, J.P. Gustafsson, EXAFS Study on the Reactions between Iron and Fulvic Acid in Acid Aqueous Solutions, Environ. Sci. Technol. 42 (2008) 2367–2373. doi:10.1021/es072092z.
[43] A. Vilgé-Ritter, J. Rose, A. Masion, J.-Y. Bottero, J.-M. Lainé, Chemistry and structure of aggregates formed with Fe-salts and natural organic matter, Colloids Surf. Physicochem. Eng. Asp. 147 (1999) 297–308.
[44] M. Pédrot, A.L. Boudec, M. Davranche, A. Dia, O. Henin, How does organic matter constrain the nature, size and availability of Fe nanoparticles for biological reduction?, J. Colloid Interface Sci. 359 (2011) 75–85. doi:10.1016/j.jcis.2011.03.067.
[45] P.J. Swedlund, J.G. Webster, Adorption and Polymerisation of silicic acid on ferrihydrite, and its effect on arsenic adsorption, Water Res. 33 (1999) 3413–3422.
[46] T. Allard, N. Menguy, J. Salomon, T. Calligaro, T. Weber, G. Calas, et al., Revealing forms of iron in river-borne material from major tropical rivers of the Amazon Basin (Brazil), Geochim. Cosmochim. Acta. 68 (2004) 3079–3094.
[47] G. Olivie-Lauquet, T. Allard, M. Benedetti, J.-P. Muller, Chemical distribution of trivalent iron in riverine material from a tropical ecosystem: a quantitative EPR study, Water Res. 33 (1999) 2726–2734.
[48] O.S. Pokrovsky, J. Schott, B. Dupré, Trace element fractionation and transport in boreal rivers and soil porewaters of permafrost-dominated basaltic terrain in Central Siberia, Geochim. Cosmochim. Acta. 70 (2005) 3239–3260.

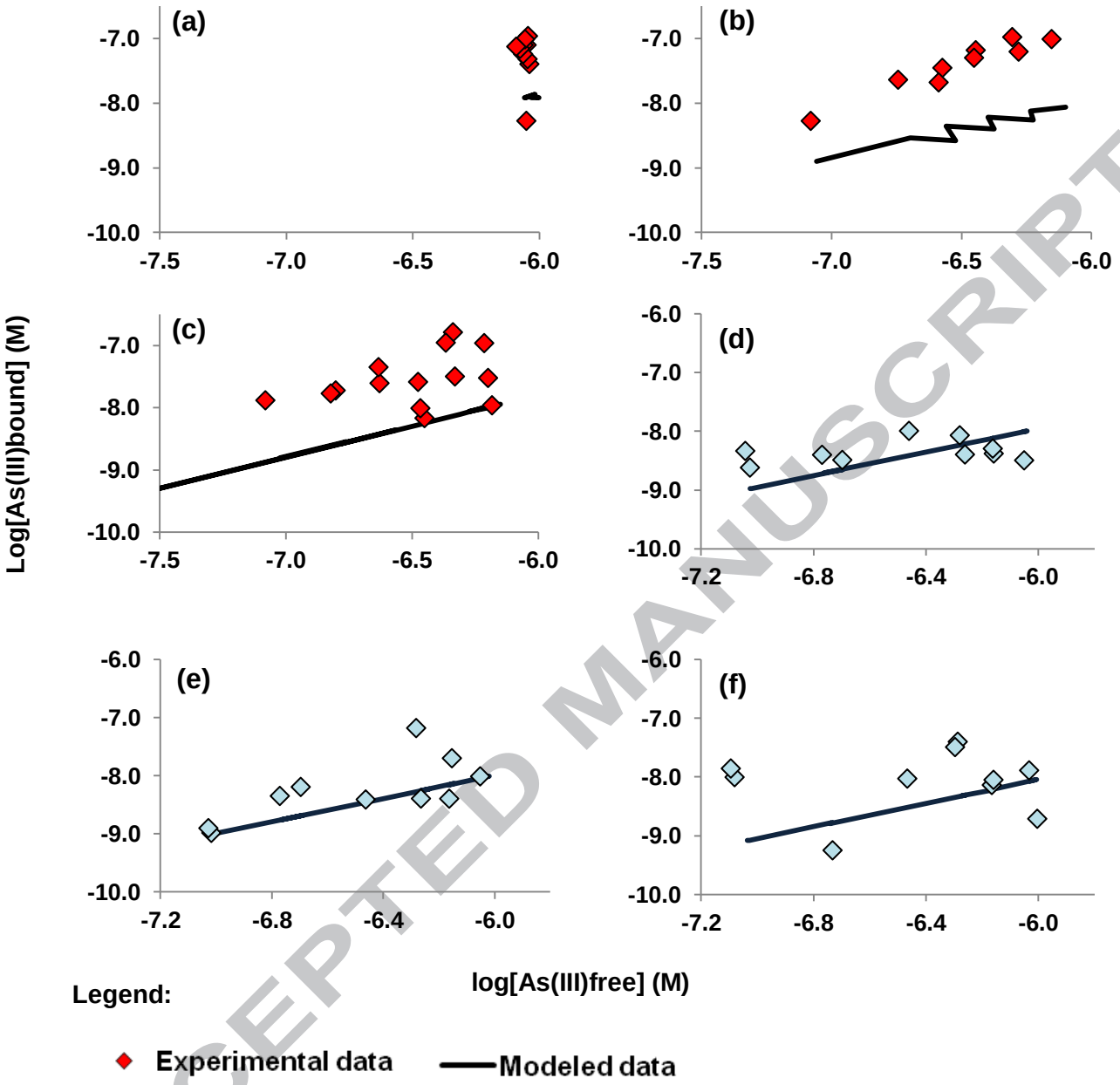

Figure 1: (a) As(III)-Fe(II)-HA binding experiments and modeled data using only the thiol binding parameters according to the [Fe(II)] concentration, (b) at pH 6, (c) pH 5, (d) As(III)-Fe(III)-HA binding experiments and modeled data using only the thiol binding parameters at pH 4, (e) pH 5, (f) pH 6.

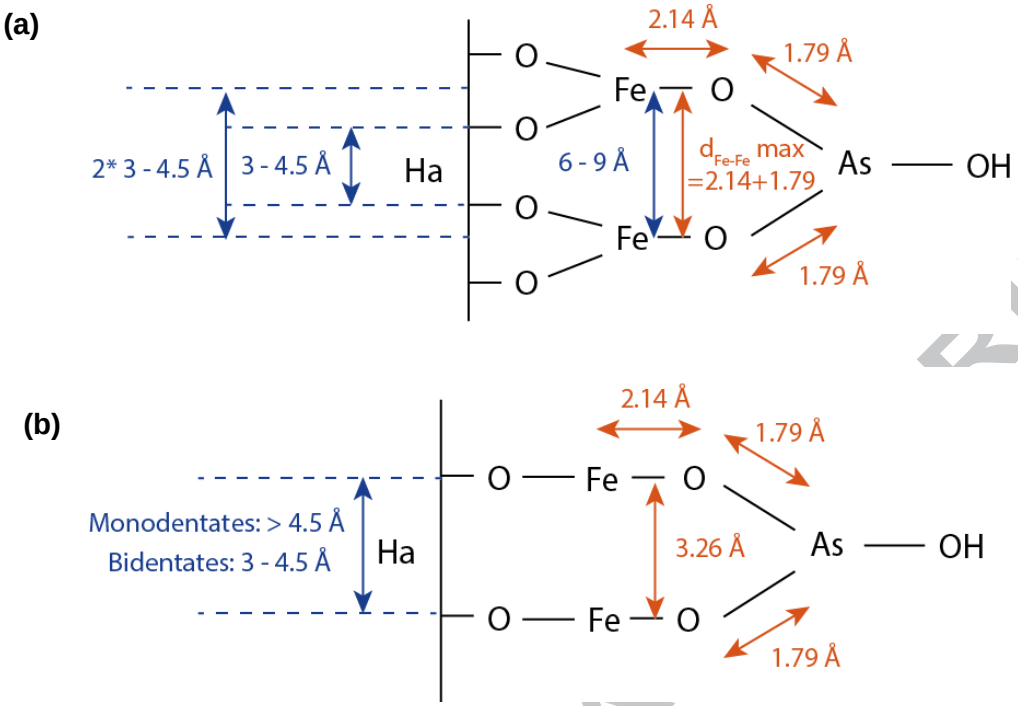

Figure 2: Complexes formed with (a) Eq. 6 and (b) Eq. 4. Fe-O and As-O distances (in red) were determined from the $Fe(OH)_2$ oxides and $As(OH)_3$, respectively [36]. The distances in blue are defined in PHREEQC-Model VI [34].

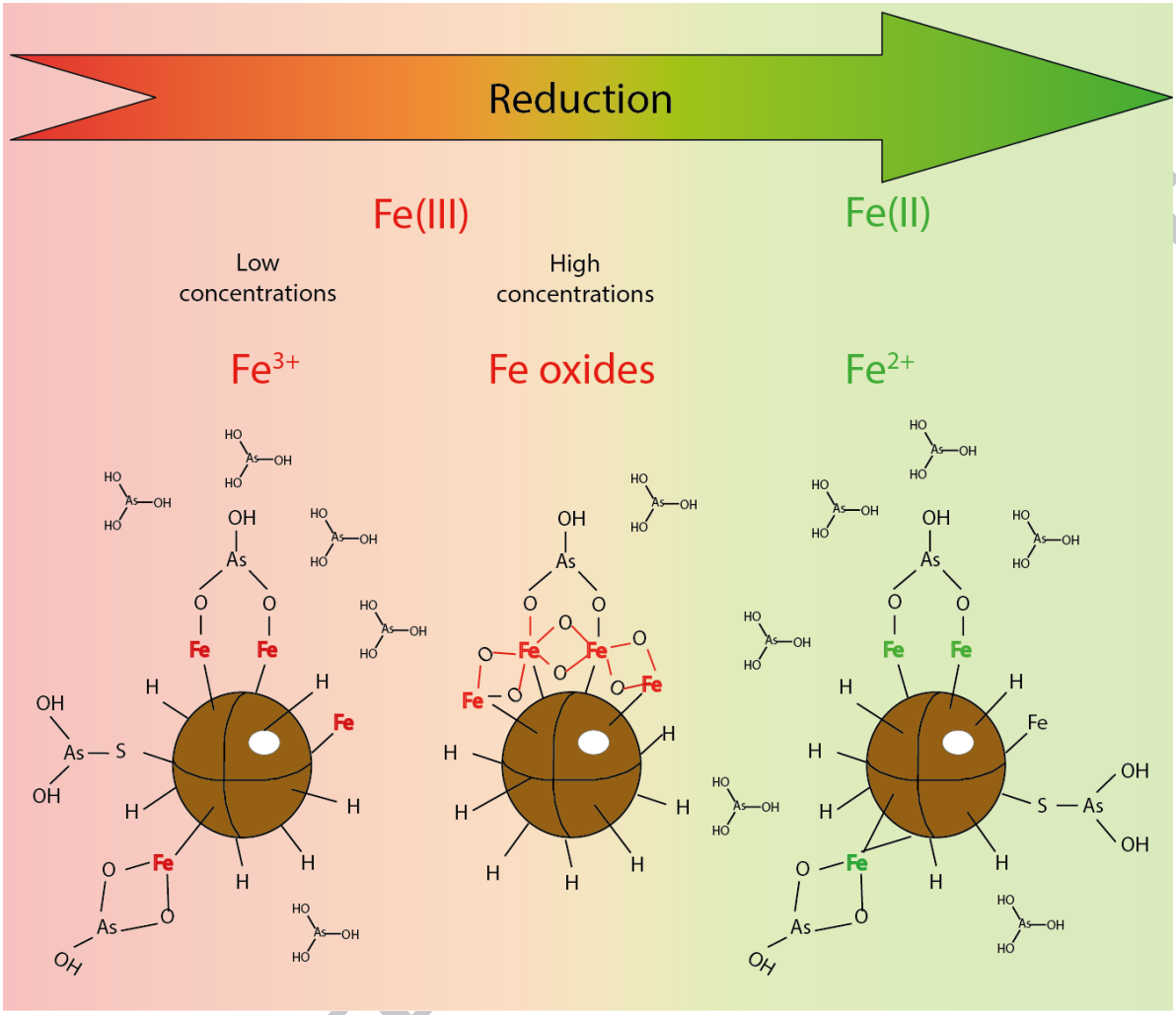

Figure 3: Schematic model describing the complexes that may form between As(III) Fe(II) and/or Fe(III) and dissolved organic matter (DOM), with regards to the redox status of Fe, and Fe and the DOM concentrations. This scheme may apply to what happens in floodplain and wetland waters [21,25,26].

Table 1: Binding parameters and RMSE for the different tested mechanisms.

Mechanism	Log k				RMSE
Eq. 1	4.15				0.38
Eq. 2	4.33				0.58
Eq. 3	3.39				0.18
Eq. 4	2.27				0.19
Eq. 1 + Eq. 2	4.15		-1.33		0.38
Eq. 3 + Eq. 4	3.39		-1.94		0.18
Eq. 1 + Eq. 2+ Eq. 3 + Eq. 4	-1.56	-1.32	3.39	-2.09	0.18

Graphical abstract